Plant Physiol. (1990) 93, 1405–1416
0032-0889/90/93/1405/12/$01.00/0

Received for publication November 1, 1989
Accepted March 7, 1990

Postphloem, Nonvascular Transfer in Citrus

Kinetics, Metabolism, and Sugar Gradients[1]

Karen E. Koch* and Wayne T. Avigne

Fruit Crops Department, University of Florida, Gainesville, Florida 32611

ABSTRACT

Postphloem, nonvascular assimilate transport occurs over an unusually long area in citrus fruit and thus facilitates investigation of this process relative to sugar entry into many sink structures. Labeled photosynthates moving into juice tissues of grapefruit (*Citrus paradisi* Macf.) slowed dramatically after entering the postphloem transport path (parenchyma cells, narrow portions of segment epidermis, and hair-like, parenchymatous stalks of juice sacs). Kinetic, metabolic, and compositional data indicated that transfer through the nonvascular area was delayed many hours by temporary storage and/or equilibration with sugars in compartments along the postphloem path. Labeled assimilates were generally recovered as sucrose throughout the path, and extent of hexose formation enroute bore no apparent relationship to the assimilate transfer process. Even after 24 hours, radiolabel was restricted to discrete, highly localized areas directly between vascular bundles and juice sacs. Postphloem transfer occurred against an ascending sucrose concentration gradient in young fruit, whereas a descending gradient (favoring diffusion/cytoplasmic streaming) developed only later in maturation. Involvement of a postphloem bulk flow is complicated in the present instance by the extremely limited water loss from juice sacs either via transpiration or fluid backflow. Nonetheless, tissue expansion can account for a collective water inflow of at least 1.0 milliliter per day throughout the majority of juice sac development, thus providing a modest, but potentially important means of nonvascular solution flow. Overall, data indicate postphloem transfer (a) can follow highly localized paths through sizable nonvascular areas (up to 3.0 centimeters total), (b) appears to involve temporary storage and/or equilibration with compartmentalized sugars enroute, (c) can occur either against an overall up-hill sugar gradient (young tissues) or along a descending gradient (near full expansion), and (d) appears to involve at least some contribution by nonvascular mass flow accommodated by tissue expansion.

Postphloem, nonvascular assimilate transfer has been difficult to distinguish experimentally from the actual process of phloem unloading. Many measures of phloem unloading necessarily include both processes (12, 27, 33). Nonetheless, these studies have demonstrated that together, phloem unloading and subsequent nonvascular transfer may contribute significantly to the regulation of source-to-sink photosynthate transport (7, 12, 27, 33). The unusual anatomical features of citrus juice tissues afford an opportunity to examine nonvascular transfer alone, over a relatively long distance, and in a system where water flow is limited.

Tissues comprising the postphloem transport path in citrus fruit are sufficiently large to allow an examination of nonvascular transfer and to clearly distinguish this process from phloem unloading. Photosynthates enroute to juice sacs arrive on the surface of a given juice segment via three major vascular bundles shown in Figure 1A, one dorsal bundle (running the length of the tangential face of each segment), and 2 septal bundles (positioned between the radial faces of adjacent segments). Following phloem unloading, ^{14}C-photosynthates move into the segment epidermis and parenchymatous, hair-like stalks of individual juice sacs (18, 21). Each juice sac stalk joins the segment epidermis at a point near one of the three major vascular strands (Fig. 1, A and B). The segment epidermis is continuous with that of the juice sac. Previous ^{14}C-labeling studies have shown that photosynthates accumulate to disproportionately high levels in this nonvascular epidermal layer, as well as the phloem-free stalks of juice sacs (18, 21). Initial analyses of structure/function relationships in these tissues indicated little specialization for transport and, in fact, showed plasmodesmatal densities in these nonvascular tissues to be similar to those of parenchyma found in many systems (21). Thus, while the nonvascular structures examined here are unusual in their length, they appear analogous in many respect to other systems.

One objective of the research described here is to clarify the relationships between sucrose metabolism, sugar gradients, and photosynthate transfer within the postphloem portion of the transport path. Plant cells which import sucrose generally do not lie immediately adjacent to the phloem, even in systems with fine vascular networks; thus, the final portion of transport must proceed through nonvascular areas of varying size. Postphloem transfer can be apoplastic (extracellular) or symplastic (cell-to-cell via plasmodesmata) (2, 4, 12, 25, 26, 33), and may involve distances ranging from a few cells (or less) to greater than a millimeter (as in cotton fibers [6], portions of some sugar beet storage rings [1], endosperm and other tissues of grains [9, 26], and citrus juice sacs [21]). Sugar gradients and sucrose metabolism may be important factors in phloem unloading and/or mass flow processes (9, 12 and

[1] Supported in part by the U.S. Department of Agriculture Competitive Research Grants Office, Photosynthesis Division, and by State and Match funds administered through the Institute of Food and Agricultural Sciences, University of Florida (U.F. Journal Series No. R-00722).

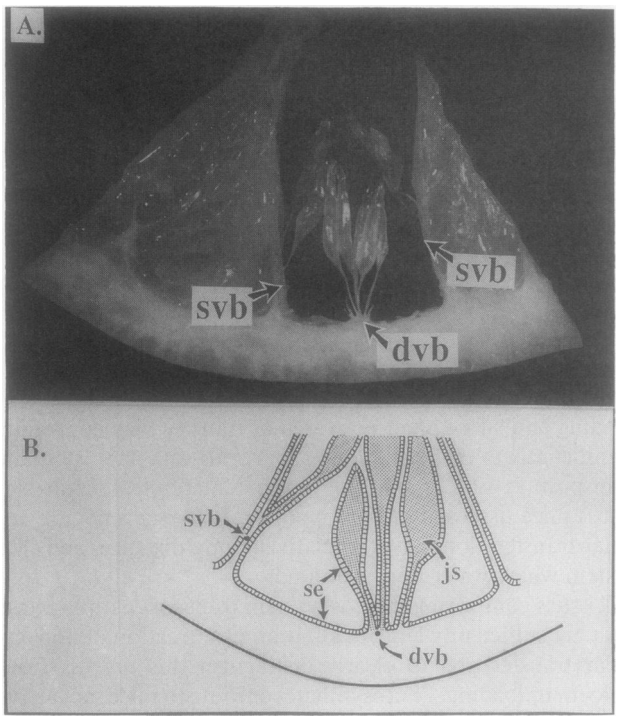

Figure 1. Position of vascular and nonvascular tissues in citrus. A, An equatorial cross-section of a grapefruit showing position of completely phloem-free juice sacs relative to major vascular strands that traverse the outer surface of each segment. Three major vascular bundles (1 dorsal [dvb] and 2 septal [svb]) supply assimilates to juice sacs of each segment, and are positioned parallel to longitudinal rows of these vesicles. B, Diagram detailing position of nonvascular segment epidermis (se) and juice sacs (js) relative to vascular bundles (dvb and svb). The multicellular juice sacs and their nonvascular, hair-like stalks join segment epidermis near the major vascular strands. Segment epidermis of each juice sac and subtending stalk is continuous with that surrounding the entire segment and immediately adjacent to the nearest vascular bundle. Distance from the site of phloem unloading to the body of juice sacs ranges of 0.2 to 1.8 cm, with the total nonvascular distance reaching 3.0 cm or greater (21; KE Koch, unpublished data).

citations therein, 27, 33). The role of these factors in relatively long-distance, nonvascular transport are examined here.

A second goal of this work is to characterize sugar transfer in a system where water movement, and hence postphloem mass flow are likely to be limited. High turgor at the sink end of a transport path can inhibit mass flow through 'back pressure' (16, 33). Juice sac turgor is typically great enough to 'stretch' thick layers of previously formed peel tissues during normal fruit development. Also, these sacs take in water slowly, and allow little or none to leave (17, 24). The vast majority of water lost from fruit by transpiration or xylem backflow appears to originate from peel tissues (24; T-B Huang, KE Koch, unpublished data). Vascular strands supplying assimilates to juice sacs are positioned in peel outside segments, leaving only the postphloem path in the zone of limited water movement. Therefore, nonvascular solute transfer into citrus juice sacs occurs without the apparent volume of bidirectional water flow typically associated with vascular sugar movement.

MATERIALS AND METHODS

'Marsh' grapefruit (*Citrus paradisi* Macf.) trees were grown in the field at Gainesville, FL, using 26 L containers. Nutrients were applied at 2- to 3-week intervals as a commercial formula (Peter's, Fogelsburg, PA) containing 10.4% (w/v) urea, 5.6% (w/v) NO_3, 4% (w/v) NH_4, 20% (w/v) H_2PO_4, 20% (w/v) K_2O, and micronutrients. Trees were 6 to 8 years old and each bore several fruit. A single, attached fruit was utilized for each replication of a given experiment. Studies were conducted about 25 to 32 weeks after fruit set, from late September to early November, when juice tissues were nearing full expansion and accumulating substantial dry matter (mean rates were typically 150 mg d^{-1} or greater for fruit of these trees during the experimental period). Field-grown trees from a commercial planting at Lake Wales, FL (130 miles south of Gainesville) provided larger numbers of fruit samples for analysis of sugar, dry weight, and water accumulation by developing juice sacs. Anthesis date and subsequent development was advanced by about 6 weeks relative to Gainesville-grown fruit, but other attributes of dry weight accumulation profiles were similar.

For radiolabel studies, a given container-grown tree was transported to the laboratory 18 h prior to $^{14}CO_2$ exposure, and a leaf nearest or next nearest a fruit was enclosed in a 46 mL acrylic plastic cuvette. During the 12 h photoperiod, temperature was 29 ± 2°C and light (400 W high-pressure sodium vapor lamp; Lucalox) was 800 to 1000 μmol m^{-2} s^{-1} PPFD. The cuvette was continuously flushed with ambient air until the start of each experiment. In pulse-chase studies, source leaves were exposed to 13.6 μCi $^{14}CO_2$ l^{-1} (50.0 μCi l^{-1} for ^{14}C-sugar studies) as described by Koch and Johnson (20), for 1 h beginning at 0800 to 1000 h the following morning. Levels of total CO_2 were maintained near those of ambient air using an infrared gas analysis system and a compressed source of $^{14}CO_2$ (20). The latter contained 372 μL L^{-1} total CO_2 and a balance of dry air. Translocation was allowed to continue for additional periods in ambient air, with each chase period lasting from 6 h to 3 weeks. Steadystate experiments were conducted for the same durations except that total $^{14}CO_2$ + $^{12}CO_2$ was maintained at levels of 150 to 425 μL L^{-1} throughout the 12 lighted hours of each period.

At the end of each experiment, radiolabeled leaves, stems, and fruit were separated, followed by dissection of the fruit quadrant in direct vertical alignment with the source leaf. This longitudinal fruit quarter typically accumulated from 84 to 96% of the ^{14}C-photosynthates translocated from a single source leaf to the fruit (19), facilitating recovery of substantial radiolabel from minute tissues. The quarter was divided into peel (pigmented flavedo and white albedo), major vascular bundles, segment epidermis, juice sacs, and hair-like stalks of juice sacs. Vascular bundles were removed from the surface of juice segments and divided into central bundles (from the innermost portion of the fruit), septal bundles (from between lateral walls of adjacent segments), and dorsal vascular bundles (one of which traverses the length of the outermost,

tangential face of each segment). Epidermis was peeled from segments, and clusters of juice sacs were frozen in liquid N_2. Individual sacs separated readily from one another when frozen, and could be detached from their respective stalks by breaking the frozen structures at the desired point with a forceps. Sample weights were determined immediately after disappearance of liquid N_2 from small weighing containers. Approximately 0.25 g of juice vesicle stalks were collected from each experiment, which required dissection of 150 to 300 juice sacs.

Samples were immediately frozen in liquid N_2 and extracted in boiling 80% (v/v) ethanol for 2 min. Tissue pieces were frozen in liquid N_2, ground to powder in a mortar and pestle, extracted a second time in cold 80% ethanol, and rinsed using Whatman No. 2 paper in a Buchner funnel. Both extracts were pooled. More than 93% of the radioactivity was released into the soluble fraction of nonleafy tissues and ^{14}C-photosynthates were quantified by standard liquid scintillation procedures.

Autoradiographs of segment epidermis and associated vascular bundles were made after 1 + 6 and 1 + 23 h pulse-chase labeling studies (as described above). Epidermis was excised intact from the segment surface, flattened, freeze dried, and exposed to x-ray film for 1 to 3 weeks at −20°C. Adjacent segments were used to quantify radiolabel in narrow strips of epidermal tissue removed at successively greater distances from vascular strands.

Sugars were separated, identified, and quantified via HPLC. Samples were homogenized for 5 to 10 min with a Polytron (Brinkman Instruments, Westburg, NY) in 5 volumes (w/v) of methanol:chloroform:water (12:5:3, v/v). Extract was filtered through Whatman No. 2 paper, rinsing insolubles with the above solution. Water and chloroform were then added to bring the final M:C:W ratio to 10:6:5. Subsequent separation of a chloroform layer allowed removal of lipids and pigments. The remaining aqueous-alcohol phase was evaporated to dryness and resuspended in a known volume of water. A 2 mL aliquot was passed through a 0.45 μm filter before injection into a Bio-Rad HPLC system (Richmond, CA). Water flowing at 0.6 mL min^{-1} was used for the mobile phase. A calcium form cation exchange column (HPX-87C, Bio-Rad) was used at 85°C and eluted peaks were detected with a refractometer (Bio-Rad). Peaks were quantified using known standards. Tissue sugar concentrations were estimated using fresh weight values from each sample to approximate fluid volume. Specific activity of each ^{14}C-sugar was determined by quantifying radioactivity in eluted fractions.

RESULTS

The primary avenues of phloem transport to developing juice sacs are three vascular strands positioned outside the segment epidermis (as in Fig. 1), and data in Figure 2A indicate that the dorsal bundle may be the most important of these. Localization and redistribution of pulse-labeled ^{14}C-photosynthates showed that after 6 h of translocation, approximately 30% of the ^{14}C-assimilates in the dissected area of the fruit were present in the dorsal vascular bundles. About half of the leaf-to-fruit transfer had been completed at this

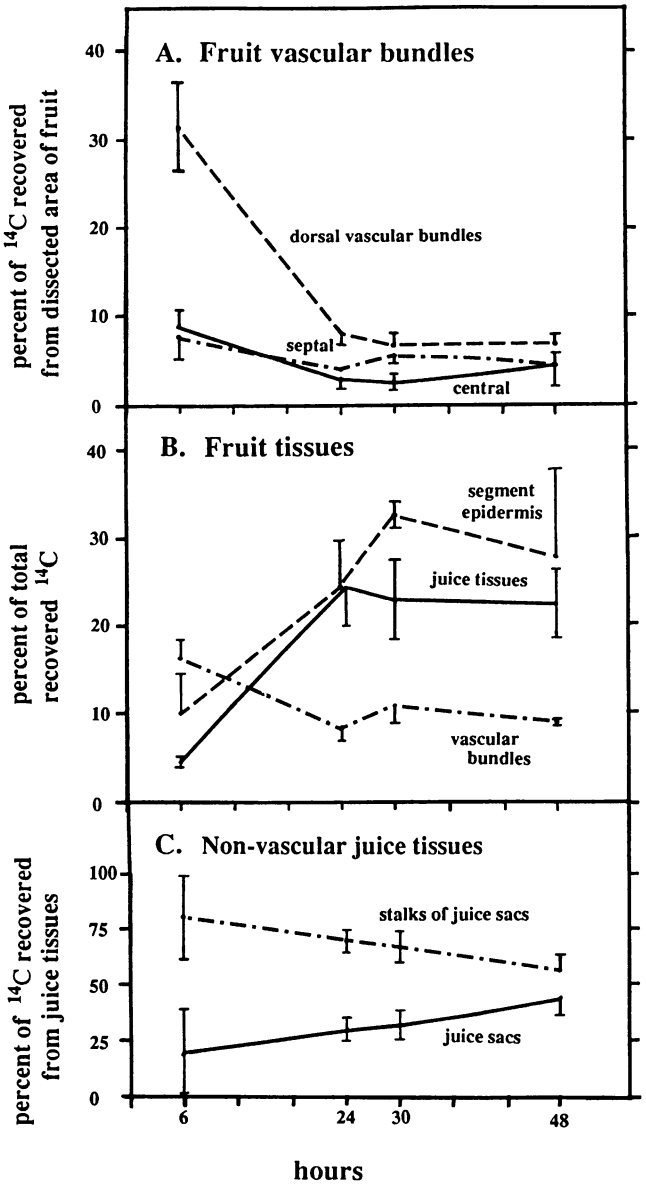

Figure 2. Kinetics of ^{14}C-photosynthate movement through vascular and nonvascular portions of the transport path in grapefruit after exposure of an adjacent source leaf to $^{14}CO_2$ for 1 h. A., Translocation through vascular bundles; B, transfer into and through vascular and nonvascular tissues to juice sacs; C, movement through final nonvascular zones of juice tissues. Fruit tissues were dissected from a longitudinal quadrant in direct vertical alignment with the source leaf. Values for B and C were calculated for whole fruit based on data from the dissected quadrant and total fruit radiolabel. A similar procedure was followed to obtain collective values for juice tissues, and was based on dissection of 150 to 300 juice sacs and their respective, subtending stalks (C). Seeds, when present, accounted for less than 2% (rarely 5%) of the total ^{14}C recovered in a given experiment. Each point represents the mean of three to four separate experiments from different trees. Vertical bars denote SEMs.

time, and most or all of the remainder (about 75% of the total recovered radiolabel) had arrived within 24 to 30 h (data not shown).

The most striking feature of Figure 2B is that by 30 h after the initial pulse of $^{14}CO_2$, the nonvascular segment epidermis contained the greatest accumulation of radiolabel, accounting for almost a third of all ^{14}C recovered from leaves, fruit, and the transport path. Amounts of label were recovered in descending order from segment epidermis, juice tissues, peel (omitted from Fig. 2B for clarity), and vascular bundles. The mean percentages of ^{14}C-photosynthates in segment epidermis dropped slightly during the interval between 30 and 48 h, indicating that subsequent export was very slow. This is consistent with the rate of dry weight accumulation by the segment epidermis at this stage (not shown).

Radiolabel in individual juice sacs compared to their hair-like stalks showed a slow but consistent transfer of ^{14}C-assimilates through phloem-free stalks and into juice sacs (Fig. 2C). However, about half of the total label in these structures remained in the parenchymatous stalks after a 48-h translocation period. At this rate of redistribution, a minimum of at least 4 d would be needed for complete transport into juice sacs. The time required for all of a 1-h radiolabel pulse to reach sites of final storage in juice sacs would be further extended by the slow transfer of assimilates from segment epidermis into stalks of juice sacs. Although some assimilates moved very slowly from segment epidermis, they were not stored for long periods according to data from 21-d experiments (distribution of radiolabel approximated that of dry matter added at the same stage [not shown]).

Continuous exposure of an adjacent leaf to steady-state levels of $^{14}CO_2$ for two successive light periods (12 h each) (Fig. 3), confirmed results of pulse-chase experiments and demonstrated that after 48 h, influx of ^{14}C-photosynthates into stalks of juice sacs proceeded more rapidly than subsequent export from stalks into sacs. The percentage of labeled assimilates in juice sacs continued to increase during this time, as is characteristic of sink structures. In contrast, the proportion of radiolabel in segment epidermis and vascular bundles remained relatively constant after the first 24 h of translocation, resembling transport and/or reservoir tissues in which rates of influx and efflux for labeled assimilates have reached equilibrium.

A revealing physical pattern of transport was evident in autoradiographs of phloem-free tissue (a localized area of segment epidermis designated in Fig. 4A is enlarged in 4B). After 24 h, a 1-h pulse of ^{14}C-photosynthates had moved away from segment vascular bundles in long, narrow peaks which terminated at discrete points where stalks of juice sacs were attached. These distances through nonvascular epidermis alone were as great as 6 mm, and marked the most direct paths to juice sac stalk attachment points. The postphloem avenue for photosynthate transfer, therefore, follows a defined and highly localized path within the otherwise uniform structure of the segment epidermis.

Segments adjacent to those used for autoradiography were dissected for quantification of radiolabel within the segment epidermis (values for fractions diagramed in Fig. 4C appear in Table I). Labeled assimilates had been translocated

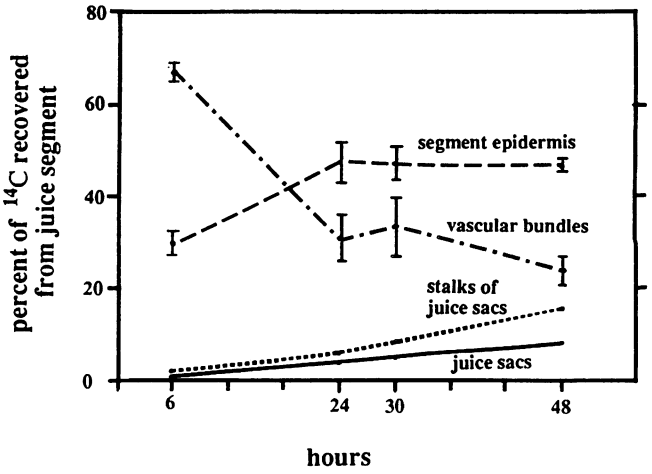

Figure 3. Kinetics of ^{14}C-photosynthate movement through vascular and nonvascular portions of the transport path in grapefruit during continuous exposure of an adjacent source leaf to steady state levels of $^{14}CO_2$ for two successive light periods (12 h light/12 h dark). Fruit tissues were dissected from the longitudinal quadrant aligned with the source leaf and found to contain 86 to 94% of the translocated radiolabel. Values for juice tissues were based on dissection of 150 to 300 juice sacs and their subtending stalks. Seeds, when present, accounted for less than 2% (rarely 5%) of the total ^{14}C recovered in a given experiment. Each point represents the mean of three to four separate experiments from different trees. Vertical bars denote SEMs.

throughout the length of the fruit within 7 h (not shown) and their distribution within vascular tissues was consistent with that shown earlier (2A). However, little radiolabel had penetrated more than a short distance into the nonvascular areas of the segment epidermis at 7 h, and Table I shows that, after 24 h, lateral movement through segment epidermis also remained limited.

Comparisons in Figure 5 show the concurrent metabolism and localization profiles for pulses of translocated ^{14}C-assimilates entering nonvascular areas, as well as total sucrose and hexose gradients obtained from the same cross-sectional samples of juice segments. Profiles of total ^{14}C-photosynthates moving into and through postphloem transport tissues were generally similar in the segments examined (Fig. 5A). Approximately one-third of the radiolabel was recovered in the narrow, nonvascular zone immediately adjacent to the dorsal vascular bundle (se1). Juice sacs and their stalks together received less than half as much ^{14}C-assimilate as was localized in the segment epidermis. The se1 samples (closest to the dorsal strand) usually contained several-fold more radiolabel than did adjacent se2 samples (not shown). Pronounced transfer of labeled photosynthates from vascular bundles to nonvascular tissues was observed in Segment 4 in Figure 5A. While unusual, such behavior is within the range observed in previous studies. This same profile was not evident in an immediately adjacent segment from the same fruit (Segment 3, Fig. 5A), demonstrating a high degree of apparent independence in radial transfer systems examined. In all instances,

however, substantially more label was localized in segment epidermis than juice sac tissues.

The extent of hexose formation was minimal for ^{14}C-photosynthates entering the postphloem transport path from dorsal vascular bundles. Generally, less than 15% of the radiolabel was recovered as hexoses in either vascular or nonvascular transport tissues. The single instance of more pronounced sucrose hydrolysis along the transport path (Segment 3, Fig. 5B) did not appear to be associated with any apparent alteration of radiolabel transfer (5A) and did not occur in an adjacent segment from the same fruit (Segment 4, Fig. 5B). Formation of labeled hexoses was also minimal in other transport tissues examined, and in the samples of segment epidermis most distant from dorsal vascular bundles (se2 fractions not pictured). Slightly greater percentages of ^{14}C-hexoses were observed at the site of final deposition (juice sacs) in most segments. This apparent breakdown of ^{14}C-sucrose (Fig. 5B) coincided with somewhat larger portions of total radiolabel transfer into juice sacs (Fig. 5A), but increased levels of ^{14}C-hexoses were detected in the sink structures rather than en route. Grapefruit often store hexoses as they near full expansion (30) and no clear relationship was evident in Figure 5 between the percentages of ^{14}C-hexoses found in the postphloem path and the efficiency of ^{14}C-assimilate transfer.

A descending sucrose gradient predominated in nonvascular tissues between sites near phloem unloading (se1) and those of assimilate deposition (juice sacs) at this stage of fruit development (near full expansion) (Fig. 5C). There was no consistent pattern of sucrose concentration between dorsal vascular bundles and nonvascular tissue; however, sucrose content in these strands represented the combined average of xylem and phloem together. Although substantial dilution of sieve tube sucrose can be assumed to arise from other phloem cells as well as xylem, values may still reflect gross differences in levels of vascular bundle sugars. These vary, but sugar content in that portion of the segment epidermis immediately adjacent to the vascular strand frequently remained greater than that of dissected bundles (se1 of Segments 1, 3, and 4, Fig. 5C). Other segment epidermis not along the immediate zone of transport (se2 positioned immediately adjacent to the se1 area) had substantially less sucrose than the other tissues sampled (not shown). Tissue hexose gradients (Fig. 5D) were similar to those of sucrose in all but one set of analyses (Segment 1), where glucose and fructose content in the storage area (juice sacs) was relatively high (late season increases in

Table I. *Distribution of ^{14}C-Photosynthates Within Segment Epidermis and Adjacent Vascular Bundles 23 h after a 1 h Exposure of the Nearest Source Leaf to $^{14}CO_2$*

Tissues are positioned as shown in Figure 4C. Values shown for lateral epidermis are limited to those nearest the vascular strands.

Portion of Segment Epidermis or Vascular Bundles		^{14}C-Photosynthate Distribution[a]		
		Stem end	Midsection	Stylar end
		(dpm tissue^{-1}) × 10^{-3}		
Dorsal tissues				
Dorsal vascular bundles[b]		274.1	519.1	1076.9
Minor veins				166.8
Interveinal epidermis		239.0	32.9	79.5
Septal tissues				
Septal vascular bundle		22.3	316.9	147.6
Interveinal epidermis			87.5	31.6
Lateral epidermis	(1)	3.0	11.0	6.8
(Position relative to vascular bundle)[c]	(2)	2.9	17.8	3.6
	(3)	6.4	8.0	5.0

[a] Data from segment positioned adjacent to that used for autoradiography in Figure 4B. [b] Major vascular bundles were sampled with segment epidermis immediately interior to the vascular strand and approximately the same width. [c] Strips of segment epidermis approximately 2 mm wide and parallel to the septal vascular bundle are numbered with increasing distance from the vascular strand. Sample (1) was positioned immediately adjacent to the septal vascular bundle.

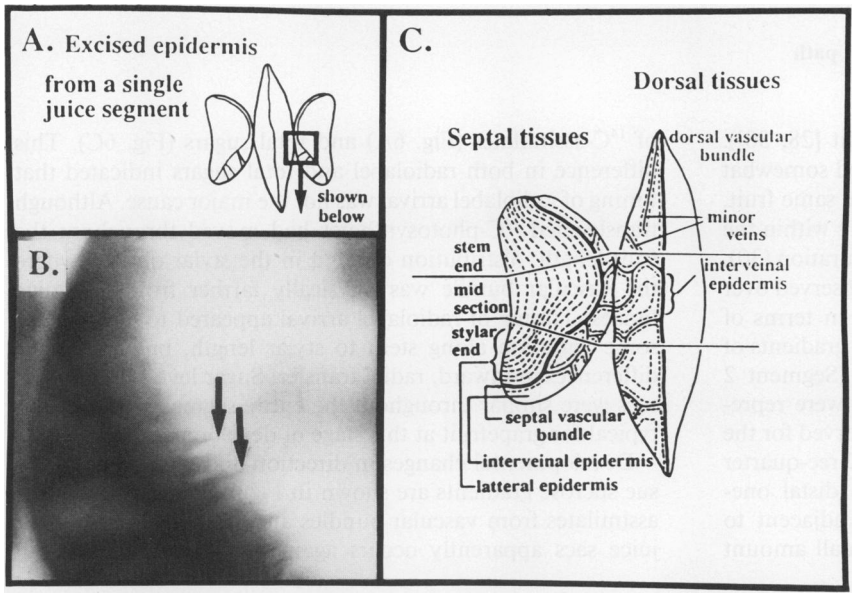

Figure 4. A, Excised whole epidermis from a single juice segment. The boxed area designates the portion enlarged in autoradiograph (B). B, Autoradiograph of excised epidermis from a single juice segment 24 h after exposure of an adjacent leaf to a 1 h pulse of $^{14}CO_2$. Radiolabeled vascular bundles on the epidermal surface appear as dark strands along the lower left. Arrows mark the points where stalks of juice sacs had been attached to segment epidermis prior to dissection. Levels of ^{14}C-assimilates were quantified in thin pieces of the adjacent segment epidermis as shown in Table I. C, Dissection diagram of segment epidermis and associated vascular tissues used for the quantification of ^{14}C-photosynthate localization and redistribution shown in Table I.

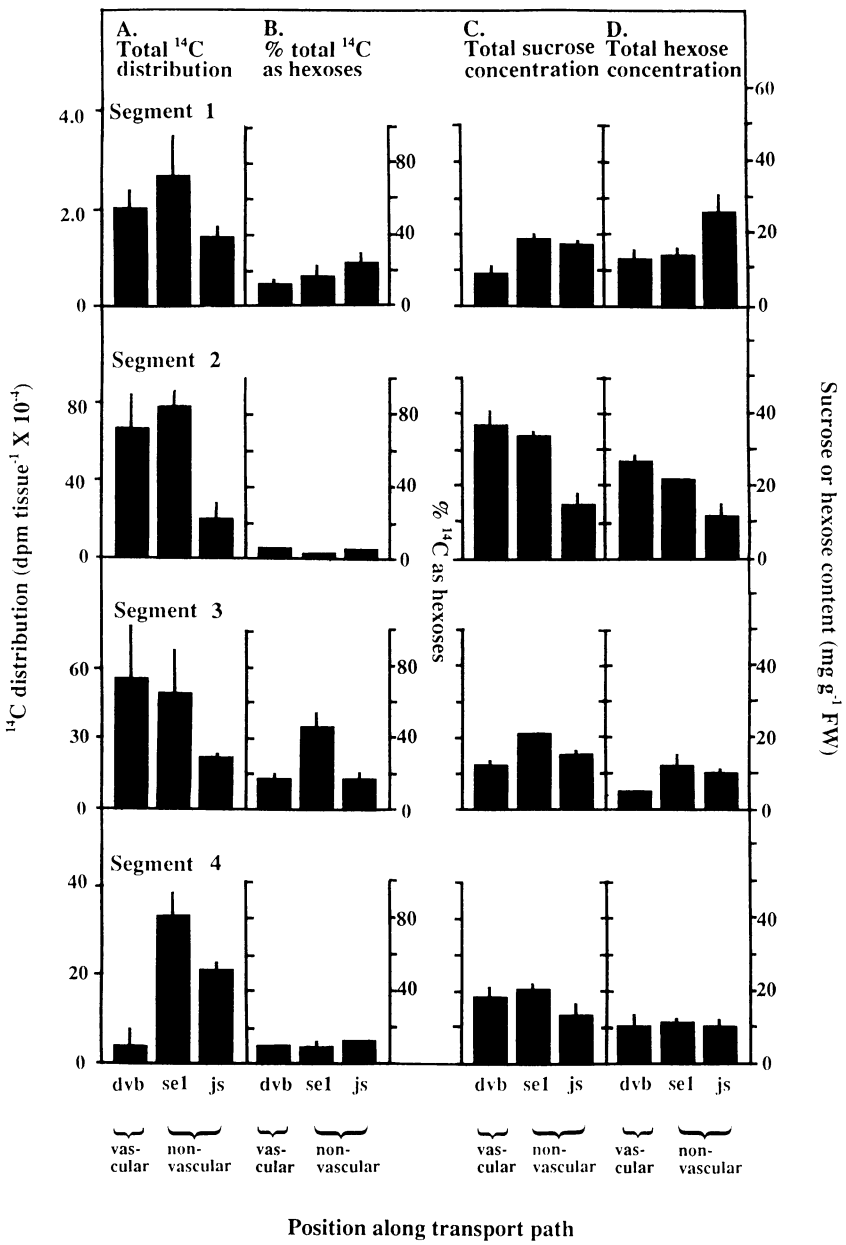

Figure 5. Simultaneous comparisons of ^{14}C-photosynthate metabolism, localization, and sugar gradients, from selected, individual transport paths through nonvascular areas in citrus fruit. A, Localization of total ^{14}C-assimilates; B, percent of tissue ^{14}C-photosynthates recovered as hexoses; C, tissue gradients of total sucrose; D, tissue gradients of total hexoses. Separate fruit were samples after experiments on three dates: September 23 (Segment 1), October 9 (Segment 2), and October 13 (Segments 3 and 4 with comparison between two adjacent segments). Values represent a radial profile along a translocation path from the dvb (dorsal vascular bundle), through the nonvascular se-1 (segment epidermis approximately 2 mm on either side of the dorsal vascular bundle), and js (juice sacs and subtending stalks attached near dorsal vascular bundles). Each value is the mean ± SEM of three separate sets of analyses, each the mean of three samples from a given cross-sectional quarter of the longitudinal axis. The entirety of a given tissue was recovered from each cross-sectional quarter (all of the segment epidermis is not pictured) and data from the proximal three-quarter (stem end) of the fruit are shown (see text and Fig. 6). Results from Segment 2 are detailed in Figure 6.

monosaccharide levels are common in grapefruit [28, 30]). The extent of sucrose and hexose gradients varied somewhat among segments, even in adjacent sections of the same fruit. However, observed sugar levels and variations are within the range of values reported for this stage of fruit maturation (30).

Generally similar translocation profiles were observed over the length of individual fruit segments (Fig. 6) in terms of total ^{14}C-distribution, ^{14}C-hexose formation, and gradients of total ^{14}C + ^{12}C-sugars. A single juice segment (Segment 2 from Fig. 5) is detailed in Figure 6, but results were representative of the within-segment relationships observed for the other juice segments examined. The proximal three-quarter fruit (stem end) consistently differed from the distal one-quarter (stylar end), where segment epidermis adjacent to vascular tissues acquired a disproportionately small amount of ^{14}C-assimilates (Fig. 6A) and total sugars (Fig. 6C). This difference in both radiolabel and total sugars indicated that timing of radiolabel arrival was not the major cause. Although translocated ^{14}C-photosynthates had moved throughout the fruit length, distribution differed in the stylar quarter where the vascular bundle was physically farther from the juice tissues. Timing of radiolabel arrival appeared to account for some variation along stem to stylar length, but not major differences in inward, radial transfer. Sugar levels in the juice sacs were similar throughout the entire segment length, as is typical for grapefruit at this stage of development (30).

Developmental changes in direction and magnitude of tissue sucrose gradients are shown in Figure 7A. Movement of assimilates from vascular bundles and segment epidermis to juice sacs apparently occurs against a pronounced up-hill

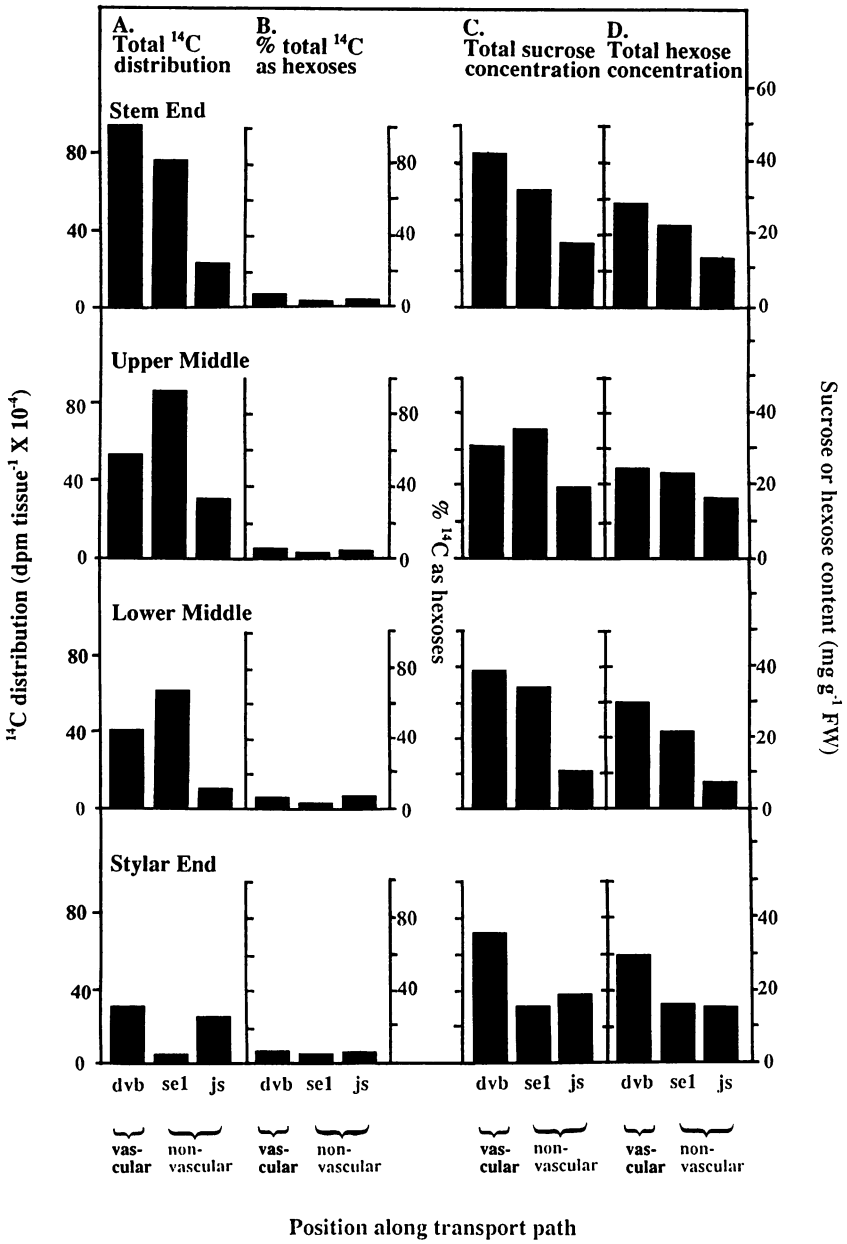

Figure 6. An expanded comparison of concurrent ^{14}C-photosynthate metabolism, localization, and sugar gradients, in the vascular and nonvascular transport path of a single segment (Segment 2 pictured in Fig. 5). A, Localization of total ^{14}C-assimilates; B, percent of tissue ^{14}C-photosynthates recovered as hexoses; C, tissue gradients of total sucrose; D, tissue gradients of total hexoses. Values represent a profile along a translocation path from the dvb (dorsal vascular bundle), through the nonvascular sel (segment epidermis approximately 2 mm on either side of the dorsal vascular bundle), and js (juice sacs and subtending stalks attached near dorsal vascular bundles). The entirety of a given tissue was recovered from each cross-sectional quarter (all of segment epidermis is not pictured). Quarter divisions are designated as the stem end (proximal to tree), upper middle, lower middle, and stylar end (distal from tree). Each value is the mean of three separate samples from a given cross-sectional quarter of the longitudinal axis.

gradient of overall sucrose levels during the first 2 to 5 months of fruit development. This also included the first portion of the 'expansion phase' of fruit growth, which takes place after completion of cell division (30). The magnitude of the ascending sucrose gradient diminished during fruit expansion. The change resulted not from juice sac sugar dilution during expansion, but from the consistent increase of sucrose level in the segment epidermis/vascular bundle fraction (se/vb). Mean sucrose concentration in the latter had risen to levels significantly greater than those of juice sacs by the end of the expansion phase for juice sacs.

The early season presence of an ascending sugar gradient between vascular areas (se/vb) and sink tissues (juice sacs) was also observed when combined levels of sucrose and hexoses were examined (no other soluble sugars were detected) (Fig. 7B). This up-hill gradient was evident for a longer portion of fruit development than was that of sucrose alone. The extent of hexose production during final phases of juice sac expansion often varies considerably under field conditions (30), resulting in total sugar gradients persisting for variable periods.

The osmotic effects of sucrose + hexoses (also in Fig. 7B) demonstrate the potential for substantial gradients in Ψ_{solute} between tissues during juice sac development. Such osmotic gradients could affect water influx and/or solute inflow. Figure 7C, for example, shows a close overall relationship between increases of fresh and dry weight in juice tissues. A more detailed analysis shows that maximal rates of juice sac water accumulation (fresh weight minus dry weight [Fig. 7D]) coincided with those of greatest dry weight increase (Fig.

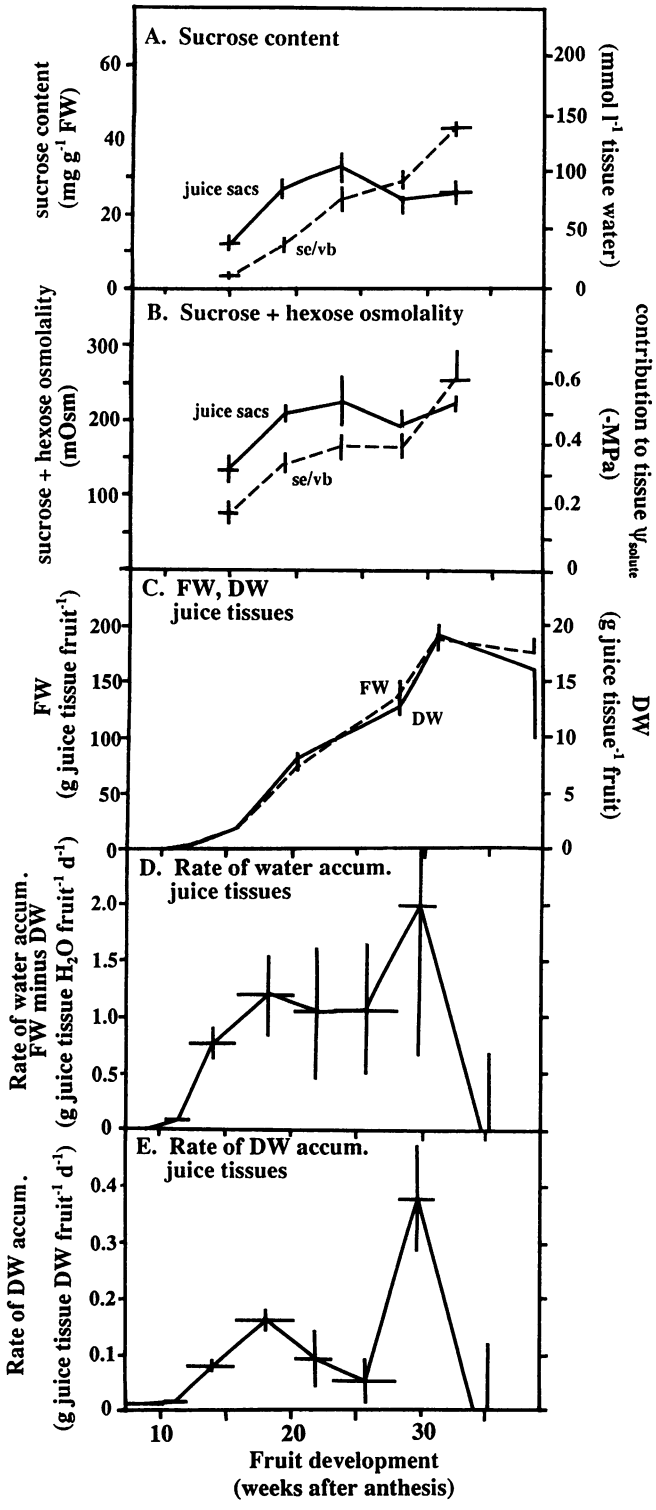

Figure 7. Developmental changes in: A, tissue sucrose gradients between transport tisuses (vascular bundle/segment epidermis fraction) and juice sacs; B, corresponding gradients in sucrose + hexose, together with their estimated contribution to tissue osmotic potential; C, fresh and dry weight gains by juice sacs; D, rates of water accumulation by juice sacs (FW [fresh weight] minus DW [dry weight]); and E, rates of dry weight accumulation by juice sacs.

7E). Both also dropped dramatically near the completion of fruit development (sugar accumulation generally continues slowly after juice sac expansion [30]). Differences between rates of water and C entry were evident, however, particularly when rising respiratory losses were included in calculations of total C demand relative to water inflow (not shown). Estimates of inflow ranged from 200 to 350 mmol during most of fruit growth (as in previous work), rising to 500 mmol or greater near full expansion.

DISCUSSION

The distinctive features of structure and water flow in citrus fruit have facilitated investigation of the relatively long-distance, nonvascular transfer of sugars, a process which occurs to varying extents in sink tissues of many species. In citrus fruit, it has been possible to distinguish this nonvascular transport process from that of the generally inclusive 'phloem unloading' studied in many systems (12, 33). Characteristics of postphloem transport have been examined over relatively long distances (>1 mm) in maize endosperm (9, 27), wheat crease/endosperm (7), rice pigment strand/nucellus (26), bean stem cortex (11, 25), epidermal hairs (31), but the size and/or structure of these areas have made it difficult to obtain complete information on the nonvascular component of the transport path. Toward this end, citrus data in the present paper compare concurrent ^{14}C-photosynthase localization, transfer kinetics, metabolism, and total sugar gradients along a phloem-free path. Key features of this nonvascular transfer are: (a) The path of sugar movement is highly localized over a relatively long distance. (b) Transport is generally slow, involves minimal sucrose hydrolysis, and appears to include equilibration and/or short-term storage with vascular sugars along the path. (c) There is a developmental shift in transfer, which initially proceeds against an ascending sugar gradient and later follows descending concentrations. (d) Maximal sugar transfer is associated with greatest apparent water flow (possible nonvascular mass flow could be accommodated to a large extent by tissue expansion).

Postphloem Path

Both pulse-chase and steady state labeling of ^{14}C-photosynthates via phloem was essentially completed within 24 to 30 h after the start of labeling, but kinetics of movement through nonvascular tissues indicated that some of the assimilates enroute to juice sacs would not arrive for at least 4 d. Others entered juice sacs more rapidly. Rates of 2.7 mm h^{-1} have been reported for nonvascular transfer through maize endosperm (27); however, comparable (but slower) movement through citrus juice sac stalks is estimated to occur only for the leading edge of ^{14}C-assimilate pulses (Fig. 2C). Delayed transfer of much radiolabel, together with the parenchymatous nature of the postphloem transport tissues, point toward temporary storage and/or equilibration of ^{14}C-sugars with pools in compartments along the nonvascular path. Vacuolar reservoirs, especially in the high-sugar areas near vascular bundles, could buffer expanding juice sacs against relatively short-term fluctuations in the supply of translocated photo-

synthates, much as proposed for parenchyma in the maize pedicel (27). Compartmentalization in vacuoles may also contribute to establishment and maintenance of sugar gradients within tissues of the postphloem transport path.

Together, the kinetic (Figs. 2 and 3) and autoradiographic data (Fig. 4; Table I) indicate that the postphloem transport path for the majority of photosynthates enroute to juice sacs is highly localized within the segment epidermis, in addition to the parenchyma of the juice sac stalks. Segment epidermis was the most heavily labeled tissue of any sampled in pulse-chase experiments (Fig. 2B) and radiolabel generally remained localized very near overlying vascular bundles at 24 h after initial exposure to $^{14}CO_2$ (Fig. 4; Table I). Eventual redistribution of the label is indicated by the attainment of essentially constant percentages of ^{14}C-photosynthates in segment epidermis during steady state labeling (Fig. 3). Moreover, the rate of dry matter accumulation in the segment epidermis was consistent with the distribution of radiolabel in long-term, 21 d translocation experiments (not shown). The autoradiograph in Figure 4B provides additional evidence for appreciable movement of ^{14}C-photosynthates through localized areas of parenchyma within segment epidermis tissues enroute to bases of juice sac stalks. The vast majority of juice sac stalks join the segment epidermis within 2 to 3 mm of the nearest vascular bundle on the tangential face of the segment, and less than 6 mm from the septal vascular bundle on the lateral face (CA Lowell, KE Koch, unpublished data).

Anatomical and ultrastructural features of this nonvascular transport path in citrus fruit show no apparent modifications for transport in either the segment epidermis or parenchyma of the juice sac stalks and zone of phloem unloading (21). Likewise, the plasmodesmatal frequency throughout juice sac stalks is also similar to that of many parenchyma tissues in sink structures of other species (21). Such a system does, however, have a theoretical capacity for symplastic transport substantial enough to supply the assimilates needed to support development of many tissues (11, 25).

Transfer of ^{14}C-Photosynthates Relative to Metabolism and Sugar Gradients

The amount of sucrose hydrolysis during/after phloem unloading (12, 27, 33) and the steepness of sugar gradients along the postphloem transport path (9, 12, 32) have both been implicated as potentially important effectors of photosynthate transfer into sink tissues. The present study addresses these relationships through a comparison of concurrent ^{14}C-photosynthate translocation, sucrose hydrolysis, and existing gradients of sucrose and hexoses in the same translocation path (Fig. 5, A–D). The nonvascular profile and portion of ^{14}C-assimilates initially reaching juice sacs was approximately similar (Fig. 5A) regardless of the amount of hydrolysis observed along the path (Fig. 5B), or of prevailing tissue sucrose of hexose gradients (Fig. 5, C and D). The two adjacent segments examined from the same fruit (Segments 3 and 4, Fig. 5A) were the least comparable in ^{14}C-assimilate delivery to juice sacs; however, differences in amounts of ^{14}C-hexose formation (Fig. 5B) or in gradients of either sucrose or hexoses were not evident (Fig. 5, C and D). Phyllotaxy of source leaves relative to individual segments can influence total amounts of labeled photosynthates transported to each (19), but is unlikely to account for obsreved differences in movement through nonvascular portions of the transport path. The lack of apparent relationship between ^{14}C-assimilate transfer and either the amount of sucrose hydrolysis in transport tissues or sugar gradients was somewhat unexpected, but is consistent with work of Fisher and Gifford (8) on transfer rates and mass flow in wheat. Additional osmotic and/or turgor considerations in the present system may be of equal or greater importance.

Sucrose Hydrolysis

Extensive sucrose hydrolysis does not seem to be directly involved in either phloem unloading or subsequent nonvascular translocation of ^{14}C-assimilates in the tissues examined here. Sink systems vary in the extent to which they hydrolyze imported sucrose, but data from maize (29) and other species (4, 22) now indicate that although cleavage and resynthesis may occur, it does not appear essential for transport. Citrus results reported here are consistent with this hypothesis.

Some formation of ^{14}C-hexoses was observed in both the vascular and nonvascular transport paths, but several lines of evidence indicate that it is not likely to be a necessary step in the direct process of assimilate transfer at the stage of fruit development examined. First, the percentage of ^{14}C-hexoses in both vascular and nonvascular transport tissues (Fig. 5B) generally was disproportionately small relative to the amount of ^{14}C-photosynthates delivered to juice sacs (Fig. 5A). Second, even if sucrose were hydrolyzed and rapidly resynthesized during transport, percentages of ^{14}C-hexoses indicate that the process occurs to approximately the same degree throughout the vascular, nonvascular, and sink tissues examined. In addition, activities of acid invertases in these tissues drop to barely detectable levels at this stage of development (23), and pH along the transport path is not likely to be low enough for rapid action of the nonenzymatic sucrose hydrolysis reported in acid limes (5). The suggestion that sucrose hydrolysis in this system is more closely related to storage than transport is also supported by the observation that instances of most pronounced formation of ^{14}C-hexoses occurred in the final storage sites (juice sacs) rather than en route. Last, and perhaps most striking, a comparison of ^{14}C-hexose/sucrose ratios (evident in Fig. 5, A and B) to their unlabeled counterparts from the same tissues (Fig. 5, C and D) shows that substantial amounts of unlabeled glucose and fructose are stored throughout the transport and sink tissues. Synthesis and storage of hexoses are known to occur in grapefruit, particularly during the last stage of fruit growth (28), so it is not surprising that this is also evident in parenchyma cells along the vascular and nonvascular transport paths. Nearly equal concentrations of unlabeled sucrose and hexoses indicated a probable, long-term equilibrium between them that was not shared by translocated ^{14}C-assimilates in the same samples. Thus, the observed production of labeled hexoses is likely to arise from those ^{14}C-photosynthates which leave the vascular and/or postphloem transport path (probably entering and equilibrating with stored vacuolar sugars)

rather than as an integral step in the post-unloading translocation process.

Sugar Gradients

Relationships between sugar gradients and assimilate transfer over relatively long distances have been difficult to explore due to limited availability of appropriate techniques and amenable plant species (3, 7, 9, 16, 32). Whole tissue concentrations can be effectively utilized if, as in the present study, samples are minute and consist of a uniform cell type (9). Each of the nonvascular juice tissues examined here were comprised exclusively of parenchyma and/or epidermal cells (21). Although dorsal vascular bundles were more complex, samples do delineate minimal values for sugar concentrations and allow comparisons between like samples.

The potential importance of sugar gradients along the transport path is three-fold. The first is noted by Fisher and Gifford (7), who propose that those regions of the pathway where gradients are steepest may be indicative of 'major resistances and/or possible control points for transport into the sink.' This suggestion is supported by present data on fruit near full expansion, where greatest ^{14}C-accumulation occurred at the high end of the steepest gradient measured (from narrow areas of segment epidermis to juice sacs). This postphloem gradient was also considerably steeper (and associated transport slower) than that observed along the vascular path (compare postphloem gradients to those in sequential vb samples from stem to stylar end in Fig. 6C).

The second implication of data on sugar gradients (Fig. 7, A and B) is that diffusion/cytoplasmic streaming becomes a more likely contributor to postphloem transfer during final phases of growth. A descending gradient of tissue sucrose appeared near completion of fruit expansion and resulted from sucrose buildup in tissues nearest the vascular bundles (Fig. 7C). Thin strands of segment epidermis at the source end of the nonvascular path were found to contain 5 to 20 mg g^{-1} fresh weight more sucrose than did juice sacs. The C transfer via diffusion which would be driven by these gradients were calculated using mean length of juice sac stalks (6.9 mm), mean number of cell-cell junctions along this distance (about 86), total cross-sectional areas of plasmodesmatal lumens and apoplast (21), and diffusion properties for sucrose through each. Cytoplasmic streaming was also assumed to provide rapid equilibration within a given cell, so that length of the diffusion path would be similar to that of the sum total of plasmodesmatal lengths (31). Resulting values were compared to the C flux required to support observed dry weight gains, CO_2 loss, and water accumulation by juice sacs. The maximum observed gradient within the nonvascular tissues would support an estimated diffusional flux for sucrose of 5×10^{-8} μmol s^{-1} through the apoplast, 12.4×10^{-8} μmol s^{-1} through the symplast (about sixfold greater if the entire plasmodesmatal anulus is considered open to flow), but not the 230×10^{-8} μmol s^{-1} required for observed growth. A 0.6 to 1.1 molar gradient within the symplast would be necessary, but was not suggested by the minute samples along the path. The potential for limited solution movement through the symplast (much as proposed for some nectaries [10]) could greatly enhance C flux via dual functioning of both diffusion and mass flow.

The third point of potential significance to postphloem sugar transfer is that it proceeds against an ascending gradient of tissue sugars during much of development. This observation contrasts sharply with the descending gradients reported in maize endosperm (9), root tips (32), sugar beet storage rings (12), or even citrus juice sacs later in development (Figs. 5, 6, and 7). Diffusion in the present system is not necessarily eliminated as a contributing mechanism for cell to cell transport, because extensive vacuolar storage could result in localization of the ascending step at only the tonoplast. More importantly, however, the osmotic contributions of sugars in young juice sacs could favor water influx and tissue expansion (given appropriate cell wall status [3]). This, in turn, could facilitate a limited amount of nonvascular bulk flow of solutes into juice sacs as long as volume increase continued.

Water Movement

Curious attributes of water movement in the present system seem to both favor and limit contributions by mass flow to solute transfer through nonvascular zones. On the positive side are, first, the ascending sugar gradients noted above. These are typically reflected in overall osmotic potentials of the respective fruit tissues (17), and are therefore conducive to water inflow and tissue expansion wherever cell wall properties allow (3). This water influx occurred at rates of 1.0 to 2.0 mL d^{-1} for the collective volume of juice sacs throughout the majority of fruit development (Fig. 7D) and could, therefore, provide a minimal, but expedient, means of at least some solute transfer across a relatively long nonvascular distance. Second, a fairly close relationship is observed between accumulation of fresh and dry weight (Fig. 7C), which should occur if mass flow is involved (14). Maximal dry weight accumulation here coincided with maximal water influx, and rate of carbon entry dropped precipitously as fruit entered the postexpansion phase of development (Fig. 7, D and E). These similarities in water and C movement imply a mass flow, but differences between them (a developmental rise in estimated C/H_2O) inflow [see discussion on sugar gradients]) favor late season contribution by diffusion/cytoplasmic streaming.

Further, a special problem for nonvascular mass flow in this system may lie in the high turgor of juice sacs, and their unusual capacity for water retention. A descending turgor gradient is essential to models of mass flow in the phloem (12) and would also be expected if some type of pressure-driven mass flow occurred through the postphloem symplast (10). High turgor at the sink end of a mass flow path may exert a 'back pressure' on transport (12, 16, 33). Counter to this is the need for particularly high turgor during juice sac expansion, because inner tissues of citrus fruit (like those of *Litchi* [13]) appear to expand only when pressure potentials rise high enough to overcome physical restriction of peel. Juice sac water (and presumably cell turgor) is also retained even under conditions of rapid transpiration by adjacent peel (17, 24). In addition, water will be drawn from peel, but not juice sacs, by transpiration of nearby leaves (24). Finally, studies with tritiated water have shown that extremely little

fluid is cycled back out of juice sacs (T-B Huang, KE Koch, unpublished data). Tissue expansion may thus be vital to nonvascular transfer in such a system, both for release of turgor (allowing mass flow and/or effective sugar compartmentalization [12, 33]) and for physical accommodation of solute entry.

Data shown here, together with the curious water-flow attributes of this system, indicate that tissue expansion alone, in continuously expanding sink tissues, can accommodate at least partial contribution to solute transfer by a postphloem mass flow. First, a simple unidirectional inflow could be maintained by tissue enlargement, much the same way as a balloon expands. Citrus juice sacs and many other minimally transpiring structures continue to expand at substantial rates for extended periods. In citrus, sucrose would need to enter sacs at estimated levels of about 200 mmol (possibly up to 350 mmol) throughout most of fruit growth to maintain observed rates of dry weight increase and CO_2 loss (21, and data not shown). These would rise to 650 mmol or greater as expansion neared completion, but development of descending gradients would favor increased involvement of diffusion/cytoplasmic streaming at this stage. The second possibility is that bulk movement of more dilute solutes may occur in conjunction with small amounts of bidirectional flow. The tissues involved are structurally uniform, but influx and limited efflux could be divided between symplast and apoplast (as proposed for wheat [15]), or between epidermis and underlying parenchyma (as indicated for rice nucellus [26]), or possibly between endoplasmic reticulum and the cytoplasmic anulus of plasmodesmata (10), or even between night and day (with diurnal oscillations in waterflow [17]). Extremely little water appears to leave juice sacs, however (17, 24; T-B Huang, KE Koch, unpublished data), so the above means of backflow potentially may be more important to water recycling within these structures. In either instance, postphloem mass flow could contribute effectively to sugar transfer over relatively long distances.

LITERATURE CITED

1. **Artschwager E** (1926) Anatomy of the vegetative organs of the sugar beet. J Agr Res **33:** 143–176
2. **Bennett AB, Damon S, Osteryoung K, Hewitt J** (1986) Mechanisms of retrieval and metabolism following phloem unloading. *In* J Cronshaw, WT Lucas, RT Giaquinta, eds, Plant Biology, Vol 1: Phloem Transport. Alan Liss Inc, New York, pp 307–316
3. **Cosgrove D** (1986) Biophysical control of plant cell growth. Annu Rev Plant Physiol **37:** 59–64
4. **Damon S, Hewitt J, Nieder M, Bennett AB** (1988) Sink metabolism in tomato fruit II. Phloem unloading and sugar uptake. Plant Physiol **87:** 731–736
5. **Echeverria E, Burns JK** (1989) Vascular hydrolysis as a physiological mechanism for sucrose breakdown. Plant Physiol **90:** 530–533
6. **Esau E** (1977) Anatomy of seed plants. John Wiley & Sons, Inc, New York
7. **Fisher DB, Gifford RM** (1986) Accumulation and conversion of sugars by developing wheat grains. VI. Gradients along the transport pathway from the peduncle to the cavity during grain filling. Plant Physiol **82:** 1024–1030
8. **Fisher DB, Gifford RM** (1987) Accumulation and conversion of sugars by developing wheat grains. VII. Effect of changes in sieve tube and endosperm cavity sap concentrations on the grain filling rate. Plant Physiol **84:** 341–347
9. **Griffith SM, Jones RJ, Brenner ML** (1987) *In vitro* sugar transport in *Zea mays* L. kernels I. Characteristics of sugar absorption and metabolism by developing maize endosperm. Plant Physiol **84:** 467–471
10. **Gunning BES, Hughes JE** (1976) Quantitative assessment of symplastic transport of prenectar into the trichomes of *Abutilon* nectaries. Aust J Plant Physiol **3:** 619–637
11. **Hays PM, Patrick JW, Offler CE** (1987) The cellular pathway of radial transfer of photosynthates in stems of *Phaseolus vulgaris* L. Effects of cellular plasmolysis and p-chloromercuribenzene sulfonic acid. Ann Bot **59:** 635–643
12. **Ho LC** (1988) Metabolsim and compartmentation of imported sugars in sink organs in relation to sink strength. Annu Rev Plant Physiol Plant Mol Biol **39:** 355–378
13. **Huang H, Qiu Y** (1987) Growth correlations and assimilate partitioning in the arilate fruit of *Litchi chinensis* Sonn. Aust J Plant Physiol **14:** 181–188
14. **Jenner CF** (1985) Movement of tritated water and ^{14}C-labelled assimilate into grains of wheat II. Independence of entry of ^{14}C-labelled assimilate and THO. Aust J Plant Physiol **12:** 587–594
15. **Jenner CF, Xia Y, Eccles CD, Callaghan PT** (1988) Circulation of water within wheat grain revealed by nuclear magnetic resonance micro-imaging. Nature **336:** 399–402
16. **Kallarackall J, Milburn AJ** (1984) Specific mass transfer and sink-controlled phloem translocation in castor bean. Aust J Plant Physiol **11:** 483–490
17. **Kaufmann MR** (1970) Water potential components in growing citrus fruits. Plant Physiol **46:** 145–149
18. **Koch KE** (1984) The path of photosynthate translocation into citrus fruit. Plant Cell Environ **7:** 647–653
19. **Koch KE, Avigne WT** (1984) Localized photosynthate deposition in citrus fruit segments relative to source-leaf position. Plant Cell Physiol **25:** 859–866
20. **Koch KE, Johnson CR** (1984) Photosynthate partitioning in split-root citrus seedlings with mycorrhizal and non-mycorrhizal root systems. Plant Physiol **75:** 26–30
21. **Koch KE, Lowell CA, Avigne WT** (1985) Assimilate transfer through citrus juice vesicle stalks: a nonvascular portion of the transport path. *In* J Cronshaw, WT Lucas, RT Giaquinta, eds, Plant Biology, Vol 1: Phloem Transport. Alan Liss Inc, New York, pp 247–258
22. **Lingle SE** (1989) Evidence for the uptake of sucrose intact into sugarcane internodes. Plant Physiol **90:** 6–8
23. **Lowell CA, Tomlinson PT, Koch KE** (1989) Sucrose-metabolizing enzymes in transport tissues and adjacent sink structures in developing citrus fruit. Plant Physiol **90:** 1394–1402
24. **Mantell A, Goldschmidt EE, Monselise SP** (1980) Turnover of tritiated water in calamondin plants. J Am Soc Hortic Sci **105:** 741–744
25. **Offler CE, Patrick JW** (1986) Cellular pathway and hormonal control of short distance transfer in sink regions. *In* J Cronshaw, WT Lucas, RT Giaquinta, eds, Plant Biology, Vol 1: Phloem Transport. Alan Liss Inc, New York, pp 295–306
26. **Oparka KJ, Gates P** (1981) Transport of assimilates in the developing caryopsis of rice (*Oriza sativa* L.): ultrastructure of the pericarp vascular bundle and its connections with the aleurone layer. Planta **151:** 561–573
27. **Porter GA, Knievel DP, Shannon JC** (1986) Carbohydrate transfer into maize kernels. *In* JC Shannon, DP Knievel, CD Boyer,

eds, Regulation of Carbon and Nitrogen Reduction and Utilization in Maize. American Society of Plant Physiologists, Rockville, MD, pp 135–145

28. **Purvis AC, Yelenosky G** (1983) Translocation of carbohydrates and proline in young grapefruit trees at low temperatures. Plant Physiol **73:** 877–880
29. **Schmalstig JG, Hitz WD** (1987) Transport and metabolism of a sucrose analog (1'-fluorosucrose) into *Zea mays* L. endosperm without invertase hydrolysis. Plant Physiol **85:** 902–905
30. **Sinclair WB** (1984) Biochemistry and physiology of the lemon and other fruits. University of California, Division of Agriculture and Natural Resources, Riverside, CA
31. **Tucker JE, Mauzerall D, Tucker EB** (1989) Symplastic transport of carboxy fluorescein in staminal hairs of *Setcreasea purpurea* is diffusive and includes loss to the vacuole. Plant Physiol **90:** 1143–1147
32. **Warmbrodt RD** (1987) Solute concentrations in the phloem and in the apex of the root of *Zea mays*. Am J Bot **74:** 394–402
33. **Wolswinkel P** (1985) Phloem unloading and turgor-sensitive transport: factors involved in sink control of assimilate partitioning. Physiol Plant **65:** 331–339